Online distributed learning in wind power forecasting

Benedikt Sommer[1], Pierre Pinson[1*], Jakob W. Messner[1], David Obst[2]

[1] *Technical University of Denmark, Department of Electrical Engineering, Kgs. Lyngby, Denmark*
[2] *EDF R&D, Palaiseau, France*
[*] *Corresponding author: ppin@dtu.dk*

Abstract

Forecasting wind power generation up to a few hours ahead is of utmost importance for the efficient operation of power systems and for participation in electricity markets. Recent statistical learning approaches exploit spatio-temporal dependence patterns among neighboring sites but their requirement of sharing confidential data with third parties may limit their use in practice. This explains the recent interest in distributed, privacy preserving algorithms to high-dimensional statistical learning, e.g., for auto-regressive models. The few approaches that have been proposed are based on batch learning. These approaches are potentially computationally expensive while not allowing the accommodation of nonstationary characteristics of stochastic processes like wind power generation. This paper closes the gap between online and distributed optimisation by presenting two novel approaches that recursively update model parameters while limiting information exchange between wind farm operators and other potential data providers. A simulation study allows the comparison of the convergence and tracking ability of both approaches. In addition, a case study using a large dataset from 311 wind farms in Denmark confirms that online distributed approaches generally outperform existing batch approaches, while agents do not have to actively share their private data.

Keywords: Energy forecasting, Distributed optimisation, Online learning, Multivariate time series, Wind energy

1. Introduction

Following the sustained deployment of renewable energy generation capacities, especially in the case of wind energy, forecasting has received increasing interest. Accurate wind power forecasts enhance the profitability of wind farms when participating in electricity markets (Mazzi & Pinson , 2017). Power system operators rely on generation and load forecasts for the optimal scheduling of conventional generation units and operating reserves (Matos *et al.*, 2017). An overview of state-of-the-art methods for wind power forecasting is presented in Giebel & Kariniotakis (2017). While lead times ranging from hours to days have been of central focus owing to wind power participation in electricity markets, other lead times ranging from a few minutes to a week ahead (or possibly more) are of relevance to a broad range of operational and decision-making problems. The demand for accurate wind power

forecasts with very short lead times ranging from minutes to a few hours has supported the development of novel forecasting methods (Pinson , 2012; Pinson & Madsen , 2012). For very short lead times, statistical and machine-learning methods clearly dominate over methods based on numerical weather forecasts. The majority of forecasting methods only utilise local data that is recorded at the wind farm of interest. Numerous publications have shown that using high-dimensional learning methods in combination with data from surrounding sites, such as meteorological stations or wind farms, can improve forecast accuracy substantially (He *et al.*, 2014; Tastu *et al.*, 2011, 2014). Generally, this modelling approach explores and exploits spatial-temporal patterns in wind power generation. It is fairly intuitive since a propagating wind field causes lagged changes in the power production between two or more geographically dispersed wind farms. Naturally, an upwind location experiences changes in wind speed first before a downwind location that is in the trajectory of the same wind field does. Hence, using explanatory variables that are related to wind speed or power production for an upwind location helps to forecast future changes in the power production for a downwind location. These dependencies may be very complex and conditional on prevailing weather conditions (Girard & Allard , 2013). Exploiting off-site information and space-time dynamics is something that is broadly considered in environmetrics e.g. for ozone forecasting (Paci *et al.*, 2013), for the prediction of weather variables e.g. precipitation (Sigrist *et al.*, 2012), and in traffic forecasting (Min & Wynter , 2011), etc. It also shares similarities with the problem of forecasting panel data with cross-sectional dependencies in econometrics (Baltagi *et al.*, 2014).

In practice, many algorithms that exploit spatial-temporal dependencies in wind power forecasting are based on *batch learning*, i.e., based on the assumption that model coefficients are time-invariant. They hence are estimated once and for all on a training dataset (the so-called "batch" of data). The estimated coefficients are then used to issue predictions even though new data arrives sequentially. In applications where the true model coefficients are time-varying, such as in wind power forecasting due to seasonal variations in wind dynamics, as well as the environment of wind farms, using batch-learning algorithms impacts forecast accuracy negatively. An approach that is then often considered is to re-estimate the coefficients using a sliding or expanding training window whenever new data samples are available (Dowell & Pinson , 2016; Zhang & Wang , 2018). The training samples are usually weighted to control how fast the estimated coefficients adapt to changes in the dataset. However, this approach is unattractive in cases where the learning algorithm cannot efficiently re-estimate the model coefficients. Especially for high-dimensional models the time required to estimate model coefficients can be prohibitive for many applications. Computationally efficient algorithms estimate time-varying model coefficients on the fly by using recursivity, whenever a new data sample is available. We use the term *online learning* when referring to such learning algorithms. Analogously, the term offline (batch) learning refers to algorithms where the time-invariant model coefficients are estimated on a batch of training samples.

Most of the proposed online learning algorithms in the wind power forecasting literature are used in combination with models that rely on explanatory variables which are measured exclusively at the wind farm of interest. Relevant methods are presented in, e.g., Møller *et al.* (2008) and Bessa *et al.* (2012). Notable exceptions are the sparse online warped

Gaussian model of Kou *et al.* (2013) and the proposal of Messner & Pinson (2019). In the latter case, the authors described an online algorithm for high-dimensional vector autoregressive (VAR) models. A limitation is that all explanatory variables must be collected by a single agent to eventually employ that algorithm. Throughout the paper we use the term *centralised learning* when referring to situations where it is necessary to have direct access to all explanatory variables centrally in order to estimate model coefficients. Considering that wind farms are operated by competing agents and that power production data and related measurements are often deemed confidential, the requirement to collect all explanatory variables centrally brings some limitations. The unwillingness of wind farm operators to share data with third parties motivates the recent interest in *distributed learning* (and possibly *privacy-preserving*) algorithms in the field of wind power forecasting.

Distributed learning algorithms conceptually aim at relaxing this necessity of collecting all explanatory variables centrally, by decomposing a learning problem into many subproblems and one master problem. When estimating the coefficients of a forecasting model for a given wind farm of interest, for which some explanatory variables are provided by other wind farms, the distributed algorithm assigns a subproblem to each wind farm where explanatory variables are available. The model coefficients are then estimated by alternating between solving the master problem and subproblems, taking advantage of algorithm-specific variables that link the subproblems to the master problem and vise versa. With such algorithms it is no longer necessary to collect all explanatory variables centrally since the explanatory variables that are provided by other wind farms are only used in their respective subproblem. The appropriate design of distributed learning algorithms protects the explanatory variables of wind farm operators by not exposing them to others. We refer to this condition when stating that the data privacy of a wind farm operator is protected.

Today, to the best of our best knowledge, only a handful of papers have investigated distributed learning algorithms for wind power forecasting (and renewable energy forecasting, more generally). The most prominent papers all build upon the Alternating Direction Method of Multipliers (ADMM). In Pinson (2016) and Cavalcante *et al.* (2017) algorithms are developed to estimate the coefficients of an AR-X model while regularising with the LASSO. Zhang & Wang (2018) extends prior work to probabilistic forecasts but replace the L_1-penalization of the LASSO with an L_2-penalization to obtain a computationally cheaper algorithm. Unfortunately, prior distributed algorithms do not allow online learning to be performed. Therefore, to estimate time-varying coefficients it is necessary to apply the algorithms on a sliding or expanding training window while weighting the data samples. As a consequence, we aim here to close the gap between online and distributed learning methods. Our contribution consequently includes: *(i)* the development of an online ADMM version, and *(ii)* additionally proposing a mirror-descent-inspired algorithm for online distributed learning. Both have advantages and caveats to be explored through simulation studies and the application to a case study with a large real-world dataset consisting of hundreds of wind farms in Denmark.

The remainder of this paper is organised as follows. The general model and forecasting framework is introduced in Section 2. Section 3 describes an online ADMM version which we refer to as Online ADMM (OADMM). Anticipating the non-negligible computational com-

plexity of the OADMM, the computationally lighter Adaptive Distributed MIrror Descent Algorithm made Sparse (Adaptive D-MIDAS) is presented thereafter in Section 4. The inherent properties of these two approaches are analysed through a simulation study in Section 5. Thereafter, the algorithms are benchmarked on a large real-world dataset consisting of 311 wind farms in Section 6. Conclusions and perspectives for future work close the paper in Section 7.

2. Modelling and forecasting framework

2.1. From agents and their data to relevant models

Wind power generation is observed at regular time intervals at S sites. Let us write $y_{s,t}$ for the power measurement of site $s \in \Omega_S = \{s_1, s_2, ..., s_S\}$ and time stamp $t \in \{1, 2, \dots, T\}$. Power measurements are commonly normalised by the nominal capacity of the site, such that eventually, $y_{s,t} \in [0, 1]$. We restrict ourselves to AR-X models using recent power measurements as explanatory variables, in a fashion similar to the models used by Messner & Pinson (2019), Cavalcante *et al.* (2017), Pinson (2016) and Zhang & Wang (2018). However, extending such AR-X models to accommodate additional explanatory variables like wind speed for instance is straightforward. Generalisation to nonlinear modelling approaches would be more complicated. Depending on the type of data collected, it may be sensible to centre the data. Other types of transformations may additionally be considered. For instance for nonlinear and bounded processes like wind power generation, the generalized logit-Normal transformation of Pinson (2012) may render more Gaussian innovations and yield a stochastic process that is more homoskedastic. Without any loss of generality, we assume that $y_{s,t}$ are transformed power measurements.

The operator of site s_j, referred to as *central agent*, contracts a set $\Omega_S^{(j)} \subset \Omega_S \setminus s_j$ of other sites to enter a *learning agreement*. Consequently, all sites $s_i \in \Omega_S^{(j)}$ are referred to as *contracted agents*. In practice, this means that the contracted agents will support s_j in improving wind power forecasts through a distributed learning framework without exposing their explanatory variables to the central agent. The cardinality of $\Omega_S^{(j)}$ will certainly be small in practice, since it may not be of relevance for a central agent to contract a large number of sites e.g. due to the limited scale of dependence structures in space and time, and possible transaction costs. Here, for simplicity, we assume that the cardinality of $\Omega_S^{(j)}$ is $S-1$, so as to overlook the selection problem. We further assume that all contracted agents are rational and act truthfully. Therefore, we overlook the potential of malicious behaviour by assuming that the learning network design incentivises all agents to be fully collaborative (e.g. through contracts).

An AR-X model is used to link the power measured at site s_j and time t with past measurements of site s_j and the sites of the contracted agents. This gives

$$y_{s_j,t} = \beta_{s_j,0,t} + \sum_{l=1}^{L} \left(\underbrace{\beta_{s_j,l,t}\, y_{s_j,t-l}}_{\text{on-site}} + \sum_{s \in \Omega_S^{(j)}} \underbrace{\beta_{s,l,t}\, y_{s,t-l}}_{\text{off-site}} \right) + \epsilon_{s_j,t} \tag{1}$$

i.e., as a linear combination of past power measurements for all sites plus an intercept term $\beta_{s_j,0,t}$ and an innovation term $\epsilon_{s_j,t}$ with zero mean and finite variance. The scalars $\beta_{s,l,t}$ are the model coefficients for lag $l = 1, \ldots, L$ and site $s \in \Omega_S$. L denotes the order of the auto-regressive process. For simplicity, we consider that the maximum lag L is the same for the central and contracted agents, though it does not need to be. In addition a time index t is used, as it is assumed that the model coefficients are time-varying. While it may be common in the econometrics literature to assume that those coefficients follow some process e.g. autoregressive (Bekierman & Manner , 2018), we consider that these coefficients follow a random walk with varying means. They can hence be tracked with some simple form of Kalman filtering where parameters are updated recursively. This approach is common in wind power forecasting, as in the examples of Pinson (2012) and Pinson & Madsen (2012) among others.

The model in (1) has many coefficients, since a different coefficient is used for each combination of location and lagged value. This potentially leads to the need to estimate $L \times S + 1$ coefficients with $L \times S + 1$ being large. As an alternative one may parameterise the spatio-temporal dynamics of wind power generation, as commonly done in environmetrics and statistical modelling of meteorogical variables (Sigrist *et al.*, 2012). However, here, these dynamics are very complex and conditional on prevailing weather conditions (Girard & Allard , 2013). Consequently, when having access to large datasets as is common with wind power forecasting, it is possible to increase the number of coefficients to be estimated. In parallel, note that in practice many of the $\beta_{s,l,t}$ coefficients are expected to be 0, depending on the de-correlation range and prevailing wind direction. This is why we employ a fully data-driven approach to variable selection and coefficient estimation through L_1 regularisation. In addition, since we are working within an online learning framework, the resulting model coefficients are time-varying and are thus expected to capture the slow variations in wind power dynamics e.g. induced by seasons and changes in the environment of the wind farms.

For convenience we rewrite (1) in the compact form

$$y_{s_j,t} = \sum_{s \in \Omega_S} \mathbf{a}_{s,t-1} \boldsymbol{\beta}_{s,t} + \epsilon_{s_j,t} \tag{2}$$

where $\mathbf{a}_{s,t-1}$ is an horizontal vector gathering the values of explanatory variables, at time t and location s, and $\boldsymbol{\beta}_{s,t}$ is the corresponding vector of model coefficients, i.e,

$$\mathbf{a}_{s,t-1} = \begin{cases} [1,\, y_{s,t-1},\, \ldots,\, y_{s,t-L}], & s = s_j \\ [y_{s,t-1},\, \ldots,\, y_{s,t-L}], & \text{otherwise} \end{cases} \tag{3}$$

and

$$\boldsymbol{\beta}_{s,t} = \begin{cases} [\beta_{s,0,t},\, \beta_{s,1,t},\, \ldots, \beta_{s,L,t}]^\top, & s = s_j \\ [\beta_{s,1,t},\, \ldots,\, \beta_{s,L,t}]^\top, & \text{otherwise} \end{cases} \tag{4}$$

Within this modelling framework, the largest contribution to explaining the dynamics of $y_{s_j,t}$ comes from local information given by lagged values of this process. In comparison,

offsite information provides a lower contribution, though still allowing a significant improvement of forecast accuracy for short lead times (Messner & Pinson , 2019). Since most of the $\beta_{s,l,t}$ coefficients are expected to be 0, this also implies that a central agent eventually does not need to make a learning agreement with many other wind farms, hence limiting communication needs and potential contracts if distributed learning was to be remunerated.

2.2. Framework for distributed and online learning

When estimating the model coefficients of such an AR-X model in a centralised setup, an agent is required (most likely the operator of site s_j, i.e., the central agent, or the contracted forecast vendor) to gather all explanatory variables. In a distributed learning network, however, the coefficient estimation problem is decomposed into many subproblems that are solved by the agents who entered the learning agreement. In our case the problem is conveniently decomposed across all S wind farm operators. The architecture of our distributed learning network is visualised in Figure 1, where the arrows indicate information exchange.

Regularly applied in distributed networks, a fusion centre (supervisory node) oversees the communication among all agents. In practice, the central agent does not directly communicate with its contracted agents, i.e., information is not directly exchanged via a peer-to-peer connection. The reason for designing the network like this is twofold. On the one hand, the communication becomes more structured for large-scale applications where each member of the learning agreement receives a forecast for its site. This requires estimating the coefficients of at least S models in parallel. On the other hand, it may support some of the privacy concerns of wind farm operators who do not wish their private information to be exposed to other agents.

In centralised learning the flow of information is unidirectional from the contracted agents to the central agent. Distributed learning algorithm require instead a bidirectional exchange of information, as the arrows show in Figure 1. Our distributed learning algorithms require each agent to solve their assigned subproblem. This is fundamentally different from centralised learning, where only the central agent performs computations when estimating the model coefficients.

Numerous distributed and online algorithms have been proposed in the literature, though not for application in renewable energy forecasting. While first focusing on the available online versions of the ADMM it was observed that all algorithms address consensus problems, i.e., require the design matrix to be horizontally partitioned across all agents (Suzuki , 2013; Wang & Banerjee , 2012; Matamoros , 2017). Figure 2 illustrates the difference between a horizontal and vertical partitioning of the set of explanatory variables in a model like the one we use here as a basis for forecasting.

From (2), it can clearly be seen that in our forecasting problem the design matrices are naturally vertically partitionable across all S agents, i.e. each agent observes a unique subset of the whole set of explanatory variables. Horizontally partitionable datasets are found in applications where instances of the design matrix are recorded at different locations but with identical features (e.g., in clinical trials carried out across multiple hospitals). While online versions of ADMM have already been proposed for horizontally partitionable design

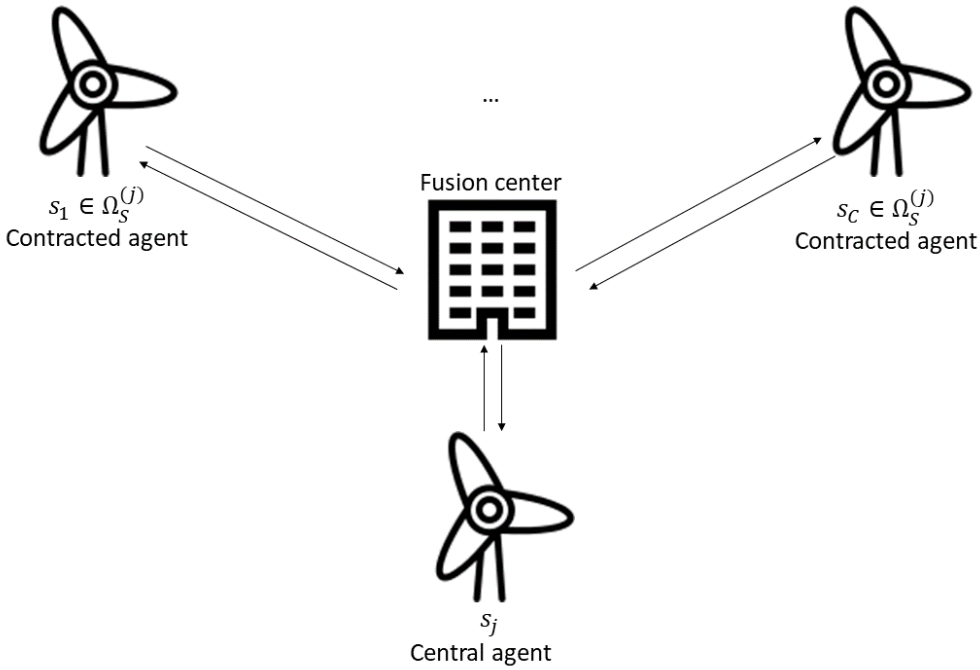

Figure 1: Architecture of the distributed learning network

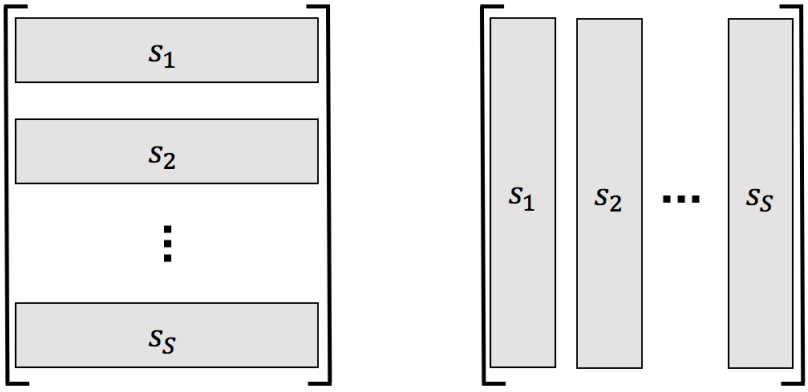

Figure 2: Horizontal (left) and vertical (right) partitioning of a matrix across S agents. Both matrices have equal dimensions. Each column represents a unique feature whereas a row is related to a time instance.

matrices, this is not the case for vertically partitionable ones. This motivates our proposal asdescribed in the following section.

3. Online Alternating Direction Method of Multipliers (OADMM)

Pinson (2016) originally proposed using the ADMM (Boyd *et al.*, 2010) to estimate the AR-X model coefficients in (1) in a distributed fashion while applying L_1-regularisation with the LASSO. The applied ADMM estimates the model coefficients on a batch of training

samples and does not allow for efficient coefficient re-estimates in applications where the true coefficients are expected to be time-varying. We thus extend this algorithm to an online version that minimises the cumulative loss over all observed data samples. Our online version efficiently re-estimates all model coefficients through recursions whenever a new data sample is available. A flowchart for the Online ADMM approach (abbreviated OADMM) is presented in Figure 3, and a detailed algorithm is available in Appendix A.

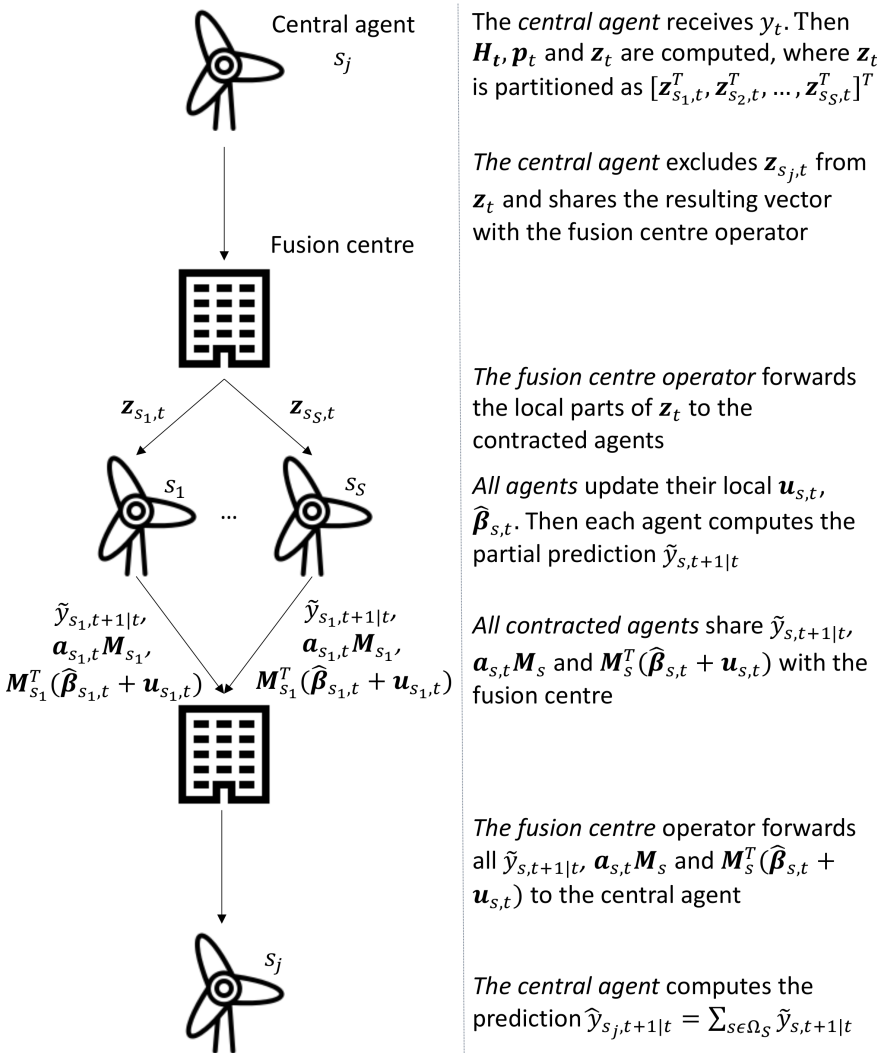

Figure 3: Flowchart for the Online ADMM (OADMM) approach for online distributed learning applied to wind power forecasting.

3.1. Coefficient estimation through a time-varying optimisation problem

Considering 1-step ahead forecasting the OADMM approach solves an unconstrained minimisation problem. For every time stamp t, it can be formulated as

$$\min_{\{\boldsymbol{\beta}_{s,t}\}_s} \frac{1}{2} \sum_{\tau=1+L}^{t} \left(\sum_{s \in \Omega_S} \boldsymbol{a}_{s,\tau-1} \boldsymbol{\beta}_{s,t} - y_{s_j,\tau} \right)^2 + \lambda \sum_{s \in \Omega_S} \|\boldsymbol{\beta}_{s,t}\|_1 \tag{5}$$

where $\boldsymbol{a}_{s,\tau-1}$ and $\boldsymbol{\beta}_{s,t}$ are as defined in (3) and (4). In parallel, $\lambda \geq 0$ is the L_1 regularisation parameter that controls sparsity. L_1 regularisation penalizes the model coefficient absolute values and thereby shrinks coefficients deemed to be insignificant towards 0.

In order to solve the minimisation problem in (5) every time a new data sample is made available, it should be made computationally efficient. Additionally, we want to control the level of adaptivity via a forgetting factor as also done by Messner & Pinson (2019), Møller *et al.* (2008) and Pinson & Madsen (2012). By giving less weight to older data, the model coefficient estimates better reflects the recent dynamics in the time-series data. Introducing an exponential forgetting factor ν into (5) results in

$$\min_{\{\boldsymbol{\beta}_{s,t}\}_s} \frac{1}{2} \sum_{\tau=1+L}^{t} \nu^{t-\tau} \left(\sum_{s \in \Omega_S} \boldsymbol{a}_{s,\tau-1} \boldsymbol{\beta}_{s,t} - y_{s_j,\tau} \right)^2 + \lambda \sum_{s \in \Omega_S} \|\boldsymbol{\beta}_{s,t}\|_1 \tag{6}$$

where $\nu \in]0, 1]$. A value of 1 results in no forgetting while decreasing values increase the amount of forgetting. Values slightly less than 1 are generally preferred. ν may be optimised in practice through, e.g., cross-validation.

The standard ADMM builds on the dual-ascent method, which is used to solve optimisation problems where the objective function is separable, by splitting the complete model coefficient vector into sub-vectors. Our problem is naturally separable since each wind farm operator has unique explanatory variables $\boldsymbol{a}_{s,\tau-1}$ and related model coefficients $\boldsymbol{\beta}_{s,t}$ in (6). The optimisation problem is transformed into an appropriate ADMM sharing form by adding the auxiliary vector $\boldsymbol{z}_{s,t}$ to (6). The constrained optimisation problem then reads

$$\begin{aligned} \min_{\{\boldsymbol{\beta}_{s,t}\}_s} \quad & \frac{1}{2} \sum_{\tau=1+L}^{t} \nu^{t-\tau} \left(\sum_{s \in \Omega_S} \boldsymbol{a}_{s,\tau-1} \boldsymbol{z}_{s,t} - y_{s_j,\tau} \right)^2 + \lambda \sum_{s \in \Omega_S} \|\boldsymbol{\beta}_{s,t}\|_1 \\ \text{subject to} \quad & \boldsymbol{\beta}_{s,t} - \boldsymbol{z}_{s,t} = 0, \quad \forall s \in \Omega_S \end{aligned} \tag{7}$$

The ADMM uses the augmented Lagrangian to solve the constrained optimisation problem with respect to $\boldsymbol{\beta}_{s,t}$ and $\boldsymbol{z}_{s,t}$, by updating the variables in an alternating fashion. For a detailed description of the ADMM and its application in distributed networks, the reader is referred to Boyd *et al.* (2010). When following the standard ADMM to solve (7), the central agent may be able to retrieve the explanatory variables of all contracted agents. Thus, the data privacy of the contracted agents is violated. In the offline ADMM for distributed learning of Pinson (2016), the explanatory variables $\boldsymbol{a}_{s,\tau-1}$ of each agent are protected in each step of the algorithm naturally by being multiplied by the respective $\boldsymbol{\beta}_{s,t}$. Taking this

as inspiration, our idea is to introduce the encryption matrix $\boldsymbol{M}_s \in \mathbf{R}^{L,L}$ and multiply it by $\boldsymbol{a}_{s,\tau-1}$ whenever it appears. We achieve this by changing the affine constraint in (7) into

$$\boldsymbol{\beta}_{s,t} - \boldsymbol{M}_s \boldsymbol{z}_{s,t} = 0, \quad \forall s \in \Omega_S \tag{8}$$

and additionally adjusting the objective function by replacing the term $\boldsymbol{a}_{s,\tau-1}\boldsymbol{z}_{s,t}$ with $\boldsymbol{a}_{s,\tau-1}\boldsymbol{M}_s\boldsymbol{z}_{s,t}$. As a requirement, each encryption matrix must be non-singular and chosen by each agent privately. This eventually yields the encrypted version of the constrained optimisation problem (7), i.e.,

$$\begin{aligned} \min_{\{\boldsymbol{\beta}_{s,t}\}_s} \quad & \frac{1}{2} \sum_{\tau=1+L}^{t} \nu^{t-\tau} \left(\sum_{s \in \Omega_S} \boldsymbol{a}_{s,\tau-1} \boldsymbol{M}_s \boldsymbol{z}_{s,t} - y_{s_j,\tau} \right)^2 + \lambda \sum_{s \in \Omega_S} \|\boldsymbol{\beta}_{s,t}\|_1 \\ \text{subject to} \quad & \boldsymbol{\beta}_{s,t} - \boldsymbol{M}_s \boldsymbol{z}_{s,t} = 0, \quad \forall s \in \Omega_S \end{aligned} \tag{9}$$

The augmented Lagrangian of (9) in its scaled form is then written as

$$\begin{aligned} \mathcal{L}_\rho(\boldsymbol{\beta}_t, \boldsymbol{z}_t, \boldsymbol{u}_t) = \frac{1}{2} \sum_{\tau=1+L}^{t} \nu^{t-\tau} \left(\sum_{s \in \Omega_S} \boldsymbol{a}_{s,\tau-1} \boldsymbol{M}_s \boldsymbol{z}_{s,t} - y_{s_j,\tau} \right)^2 + \lambda \sum_{s \in \Omega_S} \|\boldsymbol{\beta}_{s,t}\|_1 \\ + \frac{\rho}{2} \sum_{s \in \Omega_S} \|\boldsymbol{\beta}_{s,t} - \boldsymbol{M}_s \boldsymbol{z}_{s,t} + \boldsymbol{u}_{s,t}\|^2 \end{aligned} \tag{10}$$

where $\rho > 0$ is a penalty parameter and $\boldsymbol{u}_{s,t}$ are the dual variables for the constraints in (9). The OADMM then performs the minimisation of the augmented Lagrangian by sequentially optimising for $\boldsymbol{\beta}_{s,t}$ and $\boldsymbol{z}_{s,t}$ while updating the dual variables $\boldsymbol{u}_{s,t}$ as part of the dual ascent algorithm. By optimising for $\boldsymbol{\beta}_{s,t}$ and $\boldsymbol{z}_{s,t}$ individually it is possible to take advantage of the separability of (10) with respect to all $\boldsymbol{\beta}_{s,t} \in \Omega_S$.

3.2. Recursive updates of parameters

3.2.1. Central agent updates

To perform an update at time t, let us first focus on the master problem of the central agent. The central agent first observes the true power production $y_{s_j,t}$ and subsequently derives the prediction error $y_{s_j,t} - \hat{y}_{s_j,t|t-1}$. The augmented Lagrangian is then minimised with respect to the auxiliary variable z. The minimisation is written as a parameter update which is carried out exclusively by the central agent. To obtain the update equations we first define

$$\boldsymbol{\beta}_{t-1} = \left[\boldsymbol{\beta}_{s_1,t-1}^\top, \ldots, \boldsymbol{\beta}_{s_S,t-1}^\top\right]^\top, \tag{11a}$$

$$\boldsymbol{z}_{t-1} = \left[\boldsymbol{z}_{s_1,t-1}^\top, \ldots, \boldsymbol{z}_{s_S,t-1}^\top\right]^\top, \tag{11b}$$

$$\boldsymbol{u}_{t-1} = \left[\boldsymbol{u}_{s_1,t-1}^\top, \ldots, \boldsymbol{u}_{s_S,t-1}^\top\right]^\top, \tag{11c}$$

$$\boldsymbol{a}_{t-1} = \left[\boldsymbol{a}_{s_1,t-1}, \ldots, \boldsymbol{a}_{s_S,t-1}\right], \tag{11d}$$

the model coefficient estimates $\hat{\boldsymbol{\beta}}_t$ at time t, and the block-wise diagonal matrix

$$\boldsymbol{M} = \operatorname{diag}\left(\boldsymbol{M}_{s_1}, \ldots, \boldsymbol{M}_{s_S}\right) \tag{12}$$

Differentiating the augmented Lagrangian with respect to $\boldsymbol{z}_t$ yields

$$\frac{\partial \mathcal{L}_\rho(\hat{\boldsymbol{\beta}}_t, \boldsymbol{z}_t, \boldsymbol{u}_t)}{\partial \boldsymbol{z}_t} = \sum_{\tau=1+L}^{t} \nu^{t-\tau} \left(\boldsymbol{a}_{\tau-1}\boldsymbol{M}\right)^\top \left(\boldsymbol{a}_{\tau-1}\boldsymbol{M}\boldsymbol{z}_t - y_{s_j,t}\right) - \rho \boldsymbol{M}^\top \left(\hat{\boldsymbol{\beta}}_{t-1} - \boldsymbol{M}\boldsymbol{z}_t + \boldsymbol{u}_{t-1}\right) \tag{13}$$

By writing

$$\boldsymbol{H}_t = \sum_{\tau=1+L}^{t} \nu^{t-\tau} \left(\boldsymbol{a}_{\tau-1}\boldsymbol{M}\right)^\top \left(\boldsymbol{a}_{\tau-1}\boldsymbol{M}\right) \tag{14}$$

and

$$\boldsymbol{p}_t = \sum_{\tau=1+L}^{t} \nu^{t-\tau} \left(\boldsymbol{a}_{\tau-1}\boldsymbol{M}\right)^\top y_{s,t} \tag{15}$$

the auxiliary vectors are updated by equating (13) to 0 and then solving for $\boldsymbol{z}_t$. Hence, the OADMM requires

$$\left(\boldsymbol{H}_t + \rho \boldsymbol{M}^\top \boldsymbol{M}\right) \boldsymbol{z}_t = \boldsymbol{p}_t + \rho \boldsymbol{M}^\top \left(\hat{\boldsymbol{\beta}}_{t-1} + \boldsymbol{u}_{t-1}\right) \tag{16}$$

to be solved for $\boldsymbol{z}_t$. Before solving the equation system, the covariance structures $\boldsymbol{H}_t$ and $\boldsymbol{p}_t$ are efficiently updated via the recursions

$$\boldsymbol{H}_t = \nu \boldsymbol{H}_{t-1} + \left(\boldsymbol{a}_{\tau-1}\boldsymbol{M}\right)^\top \left(\boldsymbol{a}_{\tau-1}\boldsymbol{M}\right) \tag{17a}$$

$$\boldsymbol{p}_t = \nu \boldsymbol{p}_{t-1} + \left(\boldsymbol{a}_{\tau-1}\boldsymbol{M}\right)^\top y_{s,t} \tag{17b}$$

Both covariance structures comprise the memory of the recursive updating process, controlled by the forgetting factor ν.

After the central agent has updated the auxiliary vectors, it shares them via the fusion centre with its contracted agents. This is considered to be a broadcasting operation where the central agent distributes local variables within the network.

3.2.2. Contracted agent updates

After each contracted agent receives its respective auxiliary vector $\boldsymbol{z}_{s,t}$, all S agents update their dual variables in parallel with the recursion

$$\boldsymbol{u}_{s,t} = \boldsymbol{u}_{s,t-1} + \hat{\boldsymbol{\beta}}_{s,t-1} - \boldsymbol{M}_s \boldsymbol{z}_{s,t} \tag{18}$$

where the update is part of the dual ascent method.

Next follows the update of $\hat{\boldsymbol{\beta}}_t$ where the augmented Lagrangian is separable across all $\hat{\boldsymbol{\beta}}_{s,t} \in \Omega_S$. Hence, the update is also carried out in parallel. Due to the L_1-norm of the

LASSO the Lagrangian is not differentiable with respect to $\hat{\boldsymbol{\beta}}_t$, though sub-differentiable. The final update then reads

$$\hat{\boldsymbol{\beta}}_{s,t} = \mathbb{S}_{\lambda/\rho}\left(\boldsymbol{M}_s \boldsymbol{z}_{s,t} - \boldsymbol{u}_{s,t}\right) \tag{19}$$

where $\mathbb{S}_{\kappa}(c)$ is a soft-thresholding operator

$$\mathbb{S}_{\kappa}(c) = \begin{cases} c - \kappa & \text{if c} > 0 \text{ and } \kappa < |c| \\ c + \kappa & \text{if c} < 0 \text{ and } \kappa < |c| \\ 0 & \text{if } \kappa > |c| \end{cases} \tag{20}$$

which is applied element-wise to the input $\boldsymbol{M}_s \boldsymbol{z}_{s,t} - \boldsymbol{u}_{s,t}$.

3.2.3. Back to the central agent

After each agent updates their model coefficient estimates $\hat{\boldsymbol{\beta}}_{s,t}$, they compute the partial prediction $\boldsymbol{a}_{s,t}\hat{\boldsymbol{\beta}}_{s,t}$ with the latest explanatory variables. Besides sharing the partial prediction with the central agent, due to the z-update the algorithm also requires each contracted agent to share $\boldsymbol{a}_{s,t}\boldsymbol{M}_s$ and $\boldsymbol{M}_s^{\top}\left(\hat{\boldsymbol{\beta}}_{s,t} + \boldsymbol{u}_{s,t}\right)$ with the central agent. $\boldsymbol{M}_s^{\top}\boldsymbol{M}_s$ are also required by the central agent but only have to be shared once.

The last step before obtaining the next prediction requires the central agent to sum all partial predictions, i.e.

$$\hat{y}_{s_j,t+1|t} = \sum_{s \in \Omega_S} \boldsymbol{a}_{s,t}\hat{\boldsymbol{\beta}}_{s,t} \tag{21}$$

Because the OADMM requires each contracted agent to share the prior stated vectors and scalar with the central agent, the central agent has access to $L^2 + L + 1$ equations for each contracted agent and time stamp. The central agent cannot retrieve the elements of $\boldsymbol{a}_{s,t}$ because the obtained equations contain $2(L^2 + L)$ unknowns. Therefore, the data privacy of the contracted agents is protected. Besides protecting the data of each wind farm operator, the OADMM requires only a single bidirectional data exchange between the central agent and its contracted agents. Taking into consideration that only low-dimensional vectors and matrices are exchanged, the algorithm is efficient communication-wise. The pseudocode of the OADMM's final version is presented in Appendix A.

Considering all 5 required algorithm parameter updates, due to their low complexity it is expected that the β-, u- and covariance structure updates can be performed efficiently and quickly. However, the z-update is more expensive because a linear system is solved which grows linearly with the number of agents S and the order of the AR process L. Therefore, for large-scale applications with hundreds or thousands of contracted agents the z-update becomes time-intensive. This motivated us to develop a computational-wise lighter algorithm which can perform all parameter updates quickly in very large learning networks as well.

4. Adaptive Distributed MIrror Descent Algorithm made Sparse (Adaptive D-MIDAS)

In the following, we first present basic concepts about stochastic gradient descent algorithms, which are of relevance to the proposal of an online distributed learning algorithm. A flowchart for the resulting Adaptive Distributed MIrror Descent Algorithm made Sparse (abbreviated to Adaptive D-MIDAS) is presented in Figure 4, and a detailed algorithm is available in Appendix Appendix A.

4.1. Basics of the SMIDAS

Stochastic gradient descent algorithms provide a great platform for designing computationally inexpensive online distributed learning methods. We derive in the following an algorithm that is greatly influenced by the work of Shalev-Shwartz & Tewari (2011). The authors proposed the Stochastic MIrror Descent Algorithm made Sparse (SMIDAS) for solving problems of the form

$$\min_{\boldsymbol{\beta}_{s_1},\ldots,\boldsymbol{\beta}_{s_S}} C\left(\boldsymbol{\beta}_{s_1},\ldots,\boldsymbol{\beta}_{s_S}\right) + \lambda \sum_{s\in\Omega_S} \|\boldsymbol{\beta}_s\|_1 \tag{22}$$

where in regression problems C is commonly the squared loss

$$C\left(\boldsymbol{\beta}_{s_1},\ldots,\boldsymbol{\beta}_{s_S}\right) = \sum_{\tau=1+L}^{T} \left(\sum_{s\in\Omega_S} \boldsymbol{a}_{s,\tau-1}\boldsymbol{\beta}_s - y_{s_j,\tau} \right)^2 \tag{23}$$

The proposal of Shalev-Shwartz & Tewari (2011) is motivated by previous work on stochastic optimisation for L_1-regularized problems. First, Duchi *et al.* (2008) described an algorithm which replaces the L_1 regularisation term in (22) with the constraint $\|\sum_{s\in\Omega_S} \boldsymbol{\beta}_s\|_1 \leq B$ and then uses a stochastic gradient projection procedure to estimate the model coefficients. Second, Langford *et al.* (2009) introduced a stochastic gradient descent algorithm where sparse solutions are obtained by truncating the model coefficients, i.e., elements in the model coefficient vector that cross 0 during a gradient step are truncated to 0. The runtime of both algorithms might grow in some situations in a quadratic way with the dimension of the feature space even though the optimal coefficient vector is very sparse (Shalev-Shwartz & Tewari , 2011). Mirror descent algorithms instead achieve a runtime which is linear in the dimension of the feature space of the problem (Beck & Teboulle , 2003). This makes them particularly suitable for high-dimensional learning. However, they do not necessarily yield sparse solutions. In a nutshell, the SMIDAS uses mirror descent updates in combination with the truncation method of Langford *et al.* (2009). Hence, the SMIDAS achieves a superior runtime compared to the algorithms of Duchi *et al.* (2008) and Langford *et al.* (2009) while still yielding sparse solutions. Based on these properties we use the SMIDAS as a starting point for the proposal of an online distributed learning approach.

In the following, we first apply the SMIDAS to learn the time-invariant model coefficients of (22). This will facilitate the understanding of the subsequent derivation of our algorithm for learning time-varying model coefficients in a distributed setting.

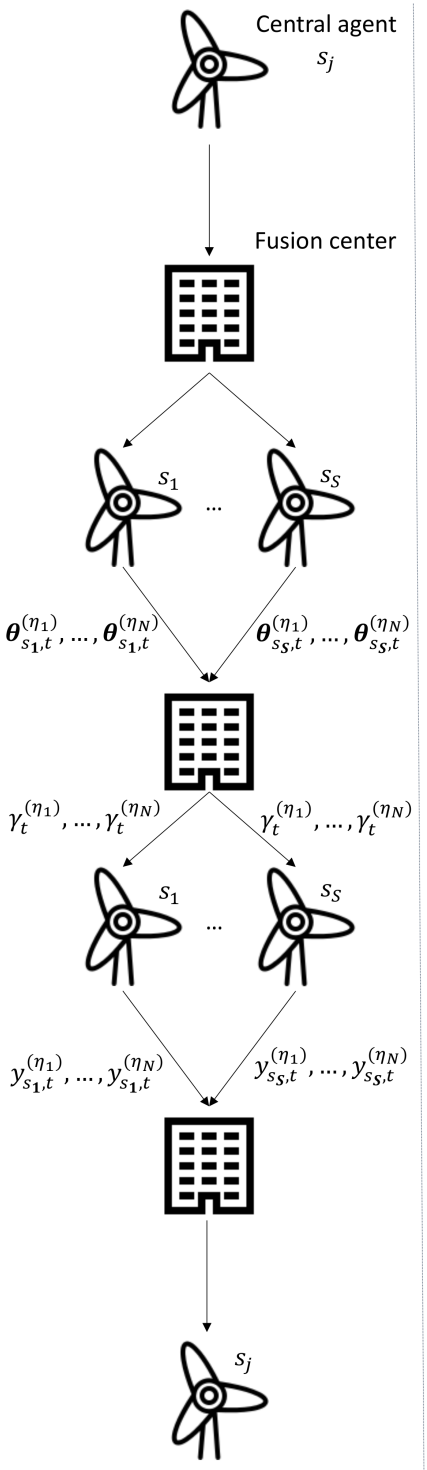

The *central agent* receives y_t. Then the forecast error $r_{t|t-1}^{(\eta)}$ and the cumulative absolute error $CAE_t^{(\eta)}$ are computed for all $\eta \in \Omega_\eta$

The central agent uses the key $\mathbb{K}$ to encrypt all $r_{t|t-1}^{(\eta)}$ and shares them then with the fusion center operator

The *fusion center operator* forwards the encrypted forecast errors to all contracted agents

After decrypting the forecast errors with $\mathbb{K}^*$, *all agents* compute the dual variables $\boldsymbol{\theta}_{s,t}^{(\eta)}$ for all $\eta \in \Omega_\eta$

All agents share all dual variables $\boldsymbol{\theta}_{s,t}^{(\eta)}$ with the fusion center operator

The *fusion center operator* computes the denominator of the link function, $\gamma_t^{(\eta)}$, for all $\eta \in \Omega_\eta$

The *fusion center operator* shares the denominators with all agents

All agents compute $\widehat{\boldsymbol{\beta}}_{s,t}^{(\eta)}$ *and* $\tilde{y}_{s,t+1|t}^{(\eta)}$ for all $\eta \in \Omega_\eta$

All contracted agents share all $\tilde{y}_{s,t+1|t}^{(\eta)}$ with the fusion center operator

The *fusion center operator* forwards all partial predictions to the central agent

The central agent computes for all $\eta \in \Omega_\eta$ $\hat{y}_{s,t+1|t}^{(\eta)} = \sum_{s \epsilon \Omega_S} \tilde{y}_{s,t+1|t}^{(\eta)}$. The prediction $\hat{y}_{s_j,t+1|t}$ is obtained as $\min_\eta CAE_t^{(\eta)}$

Figure 4: Flowchart for the Adaptive Distributed MIrror Descent Algorithm made Sparse (Adaptive D-MIDAS) approach for online distributed learning applied to wind power forecasting.

4.2. Batch estimation with SMIDAS

Like most gradient-based optimisation methods, the algorithm in Langford *et al.* (2009) updates only one weight vector $\boldsymbol{\beta}$ every iteration. Mirror descent algorithms are conceptually different because they maintain two weight vectors, the primal vector $\boldsymbol{\beta}$ and the dual vector $\boldsymbol{\theta}$. The mirror descent algorithm was first derived in Nemirovski & Yudin (1983), while a new derivation is presented in Beck & Teboulle (2003). We recommend both works for a more detailed description of the algorithm.

The two weight vectors are linked via the transformation $\boldsymbol{\theta} = f(\boldsymbol{\beta})$, where f is a link function. From the derivation in Nemirovski & Yudin (1983) and under the right conditions, f is invertible. Hence, the inverse transformation $\boldsymbol{\beta} = f^{-1}(\boldsymbol{\theta})$ exists. In Shalev-Shwartz & Tewari (2011) a p-norm link function is used, which writes

$$\beta_n = f_n^{-1}(\boldsymbol{\theta}) = \frac{\operatorname{sign}(\theta_n)|\theta_n|^{p-1}}{\|\boldsymbol{\theta}\|_p^{p-2}} \tag{24}$$

with

$$\|\boldsymbol{\theta}\|_p = \left(\sum |\theta_n|^p\right)^{\frac{1}{p}} \tag{25}$$

and θ_n being the n^{th} element in $\boldsymbol{\theta}$.

After this initial description of the mirror descent algorithm, let us apply the SMIDAS to learn the time-invariant model coefficients of (22), in a centralised setup where the central agent receive the explanatory variables from all its contracted agents.

At each iteration k, the algorithm uniformly samples a training example $i \in \{1 + L, \ldots, T\}$. Then, the gradient of the squared loss function C is estimated with

$$\nabla C\left(\hat{\boldsymbol{\beta}}_1^{(k-1)}, \ldots, \hat{\boldsymbol{\beta}}_S^{(k-1)}\right) = 2\left(\sum_{s\in\Omega_S} \boldsymbol{a}_{s,i-1}\right)^\top \left(\sum_{s\in\Omega_S} \boldsymbol{a}_{s,i-1}\hat{\boldsymbol{\beta}}_s^{(k-1)} - y_{s_j,i}\right) \tag{26}$$

where $\hat{\boldsymbol{\beta}}_s^{(k-1)}$ are the estimated model coefficients of the previous iteration and agent s. Next, the estimated gradient is used in

$$\widetilde{\boldsymbol{\theta}}_s^{(k)} = \boldsymbol{\theta}_s^{(k-1)} - \eta \nabla C\left(\boldsymbol{\beta}_s^{(k-1)}\right) \ , \quad \forall s \in \Omega_S \tag{27}$$

to update the dual variables, where $\eta > 0$ is a fixed learning rate. The SMIDAS then applies the truncation step

$$\theta_{s,j}^{(k)} = \operatorname{sign}\left(\widetilde{\theta}_{s,j}^{(k-1)}\right) \max\left(0, |\widetilde{\theta}_{s,j}^{(k-1)}| - \eta\lambda\right) \ , \quad \forall j \in \{1, \ldots, L\}, \forall s \in \Omega_S \tag{28}$$

where the regularisation strength λ pulls the dual variables towards 0. As soon as a coefficient crosses 0, it is truncated to 0. This procedure is conceptually the same as in Langford *et al.* (2009), though applied to the dual variables of the mirror descent instead of to the primal variables of the stochastic gradient descent. The last step of the SMIDAS applies the p-norm link function

$$\hat{\boldsymbol{\beta}}_1^{(k)}, \ldots, \hat{\boldsymbol{\beta}}_S^{(k)} = f^{-1}\left(\boldsymbol{\theta}_1^{(k-1)}, \ldots, \boldsymbol{\theta}_S^{(k-1)}\right) \tag{29}$$

to update the model coefficient estimates.

Equations (26) to (29) are applied until a defined convergence criterion is reached. Depending on the dataset size and convergence criterion, the algorithm can sample a single training example multiple times.

4.3. Online distributed MIDAS

The motivation to use the SMIDAS as the basis for our distributed online algorithm comes from the separability of (26) in the explanatory variables and the possibility of obtaining sparse model coefficient vectors through the truncation step (28). By choosing the loss function C as the quadratic criterion, the term $\sum_{s\in\Omega_S} \boldsymbol{a}_{s,i-1}\hat{\boldsymbol{\beta}}_s^{(k-1)} - y_{s_j,i}$ in (26) is the 1-step ahead forecast error of iteration k. Hence, if the central agent shares the forecast error for its site with the contracted agents, each agent is able to estimate their share of the gradient locally. Given the remaining steps of the SMIDAS, this allows, with a few modifications only, the obtainment of a distributed online algorithm where the privacy of each agent is protected. However, one might argue that the forecast error is a private information for the central agent, who hence is not willing to share it. In situations where the central agent is not willing to share forecast errors with competitors, we propose the following distributed learning network design. When sharing the forecast error through a fusion centre with contracted agents, the forecast error is anonymised such that the contracted agents cannot infer the identity of the central agent, and hence cannot identify the location of the related site. The anonymisation of the central agent would further require that potential compensations for the participation in a learning agreement are handled by the fusion centre operator.

To obtain a learning algorithm which is able to track time-varying model coefficients, our algorithm does not randomly sample training examples. Instead, the algorithm estimates the gradient for a sample only once as observations arrive sequentially. Therefore, the index t replaces i in all previous SMIDAS formulations. We further change the name of the algorithm to MIDAS because we remove the stochasticity by not using random samples. Last, we remove the iteration counter k (t is the equivalent in online learning) from all formulations. Estimating the gradient of a sample only once is fundamentally different from the OADMM where the cumulative loss is minimised over all past observations. This means that, when updating the model coefficients, all past information is implicitly considered. Consequently, when using the distributed MIDAS version, we expect a greater variance in the estimated model coefficients.

Starting from the willingness of the central agent to share its forecast error $r_{t|t-1} = \hat{y}_{s_j,t|t-1} - y_{s_j,t}$ with the contracted agents at time t, we propose the following distributed MIDAS. Instead of sharing the forecast error directly with the contracted agents, it is shared through a fusion centre. This is considered to be the first broadcasting step. Each agent then updates their local dual variables by taking a step into the direction of the negative estimated gradient while controlling the step size with the learning rate η. The update is performed by all agents in parallel and is written as

$$\widetilde{\boldsymbol{\theta}}_{s,t} = \boldsymbol{\theta}_{s,t-1} - \eta \boldsymbol{a}_{s,t-1} r_{t|t-1} \tag{30}$$

The SMIDAS subsequently uses the element-wise truncation (28). A simulation study revealed that a single sample evaluation does not yield significant benefits in terms of forecast accuracy. Furthermore, we realised that the p-norm link function is sufficient to shrink unimportant model coefficients to 0, though the estimated model coefficients never became exactly 0. Therefore, we dismissed the option to obtain sparse coefficient vectors by neglecting the truncation step in our distributed version (i.e., $\widetilde{\boldsymbol{\theta}}_{s,t}$ is hereafter replaced by $\boldsymbol{\theta}_{s,t}$). We subsequently obtain an algorithm that has one less hyperparameter. However, the inability to shrink unimportant model coefficients to 0 is a setback if compared to the case of OADMM.

The next step of the algorithm utilises the fusion centre, with which all agents share their dual variables. This allows the computation of the denominator of the link function with

$$\gamma_t = \|\boldsymbol{\theta}_t\|_p^{p-2} \tag{31}$$

where $\boldsymbol{\theta}_t$ is the assembly of all local dual vectors $\boldsymbol{\theta}_{s,t} \in \Omega_S$ and p is a hyperparameter. This step marks the first gathering step, even though the local variables are not gathered by the central agent. The norm γ_t is consequently shared with all agents such that they can apply the link function to their respective dual variables. This is the second broadcasting step of the algorithm. The final update is the element-wise application of the link function

$$\hat{\boldsymbol{\beta}}_{s,t} = \frac{\operatorname{sign}(\boldsymbol{\theta}_{s,t})|\boldsymbol{\theta}_{s,t}|^{p-1}}{\gamma_t} \tag{32}$$

The aforementioned shrinkage behaviour of the link function is controlled via the hyperparameter p, where a greater value in p applies a greater shrinkage to all $\hat{\boldsymbol{\beta}}_{s,t}$'s.

After obtaining re-estimated model coefficients, each agent calculates a new partial prediction and shares it through the fusion centre with the central agent, who eventually calculates the next prediction for its site. The final exchange of information accounts for the second gathering step. In total the algorithm requires 2 broadcasting and 2 gathering steps for each t.

4.4. Extending the distributed MIDAS

With the distributed MIDAS version, the fusion centre operator could have the possibility to retrieve the information about local explanatory variables. This possibility exists since the access to all dual variables and the forecast errors results in an equal amount of equations and unknowns. Therefore, additional measures are required to protect the data of the wind farm operators. Due to the different structure of the algorithms, introducing an encryption matrix as in the OADMM was unsuccessful. Our proposal is therefore to encrypt the forecast errors using an encryption technique such as AES (Li *et al.*, 2009) and then share it through the fusion centre with the contracted agents. This requires the direct exchange of the decryption key with the contracted agents before all agents start performing online learning. Because the fusion centre operator does not have access to the forecast error anymore, it has more unknowns than equations to solve. Hence, it is not possible to retrieve the explanatory variables with sufficient accuracy. In a setting with anonymized forecast errors, the central

agent still shares the decryption key with its contracted agents. However, the central agent does not reveal its identity and therefore the contracted agents cannot obtain information about the location of the central agent's site.

In the presented algorithm, named Distributed MIDAS (D-MIDAS), the learning rate η controls the general speed with which the algorithm approaches the global optimum of the minimisation problem within a given period. When η is large, the global optimum is approached faster but at the same time the estimated model coefficients experience a greater variance between consecutive time stamps. This statement is derived from (30), where a large forecast error translates directly to a significant change in the dual variables, and subsequently to a notable change in the model coefficients. Ideally, in stationary periods the algorithm requires smaller η values compared to non-stationary periods. Taking into account that all algorithm parameter updates are computationally cheap, our proposal is to learn multiple AR-X models in parallel while varying the learning rate η between the models.

Based on the past performance of each model, the algorithm adaptively chooses which model to use for the next prediction. This can considered as adaptive learning, where in stationary periods a small η is used, and in non-stationary periods a larger η is applied instead. We use the cumulative absolute error (CAE) with decaying weights

$$CAE_t^{(\eta)} = \mu CAE_{t-1}^{(\eta)} + |\hat{y}_{s_j,t|t-1}^{(\eta)} - y_{s_j,t}| \tag{33}$$

to evaluate the performance of each model, where μ allows the control of the level of decay. The superscript η indicates from which model the prediction is coming from. We name this extension Adaptive D-MIDAS and the pseudocode is shown in Appendix A.

The computational complexity and the amount of exchanged data increases linearly with the number of models that the Adaptive D-MIDAS learns in parallel. Concerning the amount of exchanged data, the Adaptive D-MIDAS exchanges an almost equal amount of data as the OADMM when learning two models in parallel. However, the Adaptive D-MIDAS requires two bidirectional data exchange steps whereas the OADMM requires only one. The additional data exchange step comes from the requirement to compute the denominator of the link function at the fusion centre. Based on this insight we obtain a communication-reduced version of the algorithm by using the denominator and dual variables of the previous time stamp to update the model coefficients via the link function. Consequently, it is no longer necessary to send the dual variables to the fusion centre before updating the weight vector. The denominator of the link function can instead be calculated after the central agent has calculated the next prediction for its site. With this strategy that reduces the overall time between obtaining the newest observation and calculating a new prediction with re-estimated model coefficients, it is expected that a negative impact on forecast accuracy will be observed. However, as the later following case study using real-world data shows, the reduction in forecast accuracy is small.

5. Simulation study

A study on simulated data investigates the ability of both algorithms to estimate time-varying model coefficients and the related computational costs. We only consider the standard Adaptive D-MIDAS and not its communication-reduced version since the lagged calculation of the denominator γ_t was verified to have only a small impact on the estimated model coefficients.

5.1. Tracking of time-varying coefficients

We first generate a multivariate time series with time-varying coefficients of the form

$$\boldsymbol{y}_t = \boldsymbol{A}\boldsymbol{y}_{t-1} + \boldsymbol{\epsilon}_t \tag{34}$$

where $\boldsymbol{\epsilon}_t$ is a vector of independent standard Gaussian noise with 0 mean and finite variance (set to 0.1 in our experiments). Each simulated time series has 25 000 times steps. The coefficient matrix $\boldsymbol{A}$ is further defined as

$$\boldsymbol{A} = \begin{bmatrix} 0.9 & 0 & 0 & 0.2 & 0 & 0 & 0 & 0 & 0 & 0 \\ 0 & 0.8 & 0.1 & 0 & 0 & 0 & 0 & 0 & 0 & 0 \\ 0 & 0 & 0.85 & 0 & 0 & 0 & 0 & -0.15 & 0 & 0 \\ 0 & 0 & 0 & 0.75 & 0 & 0 & 0 & 0 & 0 & 0 \\ 0 & 0 & 0 & 0 & a_1 & 0.2 & 0 & 0 & 0 & 0 \\ 0 & a_2 & 0 & 0 & 0 & 0.9 & 0.2 & 0 & 0 & 0 \\ 0 & 0 & 0 & 0 & 0 & 0 & 0.85 & 0 & 0 & 0 \\ 0 & 0 & 0 & -0.1 & 0 & 0 & 0 & 0.7 & 0 & 0 \\ 0 & 0 & 0 & 0 & 0 & 0 & 0 & 0 & 0.9 & 0 \\ 0 & 0 & 0 & 0 & 0.15 & 0 & 0 & 0 & 0 & 0.8 \end{bmatrix} \tag{35}$$

where a_1 and a_2 are time-varying coefficients (as illustrated in Figure 5). We performed a Monte-Carlo simulation with 1 000 replicates to estimate the variance of $\hat{a}_1$ and $\hat{a}_2$. The hyperparameters p and μ of the Adaptive D-MIDAS were set to 2.5 and 0.996, respectively. In this experiment we used 6 evenly spaced (from 0.025 to 0.15) learning rates.

Figure 5 shows the temporal evolution of the mean, as well as the $5th$ and $95th$ quantiles of the estimated coefficient distributions for a_1 and a_2. Both algorithms are able to track the time-varying coefficients in expectation (the mean of the estimated coefficient distributions follows the true values). However, some noticeable differences are observed between both algorithms. First of all, the Adaptive D-MIDAS has a greater "burn-in" period, i.e., the number of samples required to learn from before a fair approximation of the true coefficient value is reached. Secondly, the spread in the estimated model coefficients for the 1 000 replicates (represented by the difference between both quantiles) increases for the Adaptive D-MIDAS when the true coefficients change. Contrary to this, the spread in coefficient estimation for the OADMM is either constant or even decreases for changing true coefficient values. The increased spread for the Adaptive D-MIDAS coefficient estimates is a consequence of the faster learning rate which is required to keep track of the decreasing true coefficient value.

This can also be observed from Figure 6, which shows the average (over all 1 000 Monte-Carlo replicates) learning rate of the Adaptive D-MIDAS. It reveals a clear relationship

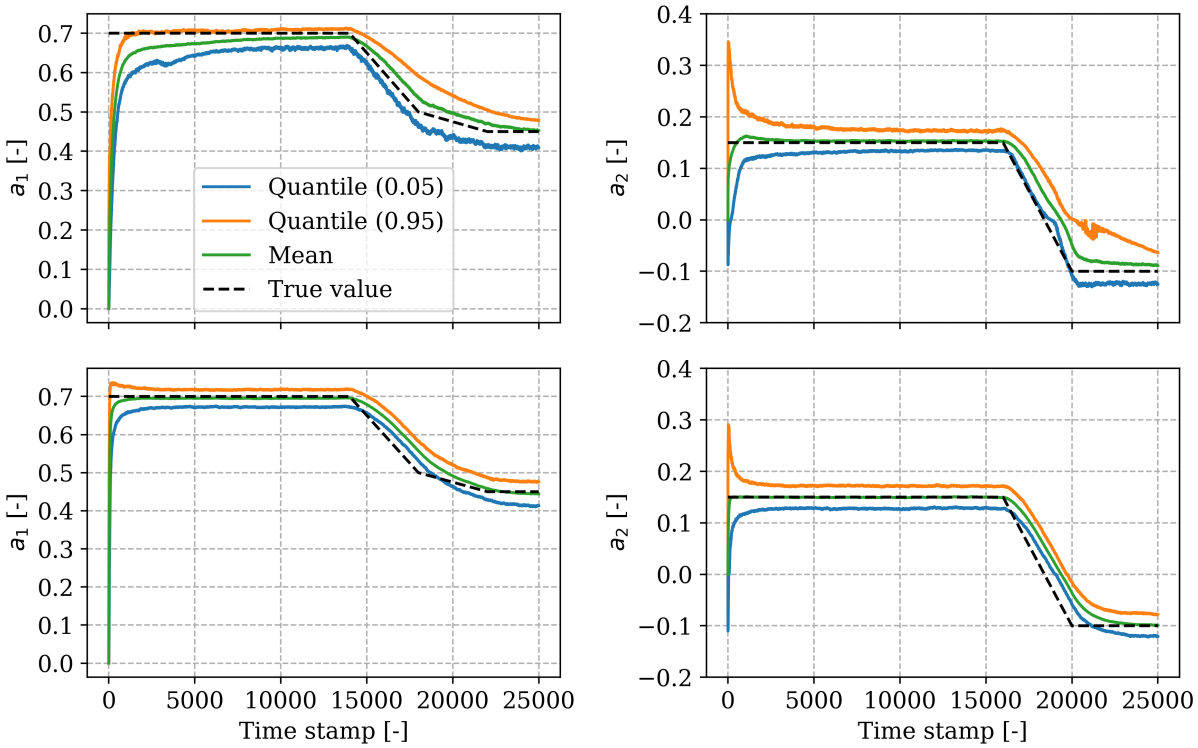

Figure 5: Coefficient estimates obtained through the Monte-Carlo simulation. Top row: Adaptive D-MIDAS, bottom row: OADMM

between the spread in the coefficient estimates and the best-performing learning rate (based on (33)).

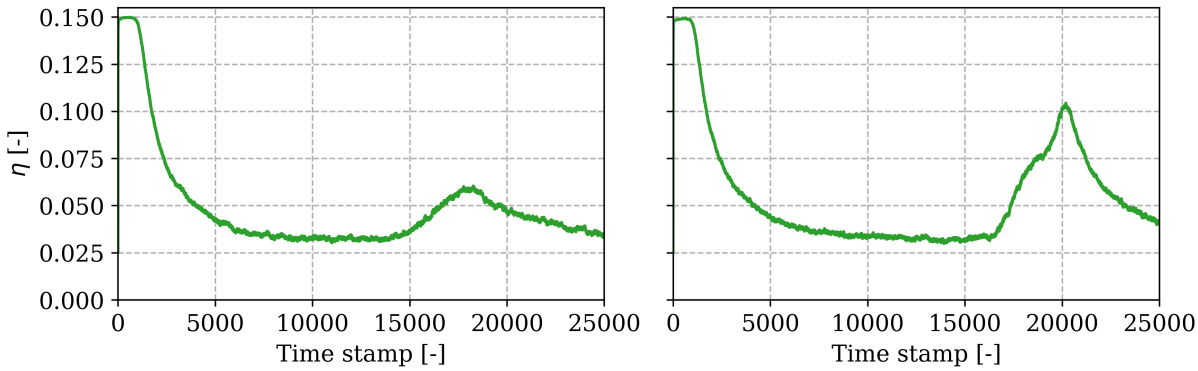

Figure 6: Average learning rate of the Adaptive D-MIDAS across all 1 000 replicates. Left a_1 right a_2

Thus, there is a clear trade-off for the Adaptive D-MIDAS between the variation in the estimated model coefficients and the ability to track time-varying coefficients: when trying to achieve a high degree of adaptivity, one has to pay the price of higher variation in the

estimated coefficients.

A similar trade-off is observed for the OADMM, where the adaptivity is controlled by the forgetting factor ν. When applying a smaller ν value, the algorithm becomes more adaptive but since the effective training data length decreases the variance in the estimated coefficient increases. However, the OADMM provides a better trade-off between adaptivity and estimated coefficient variance due to the fact that it minimises the cumulative loss over all past observations. Thus, occasional outliers in the form of large forecast errors have a smaller impact on the estimated coefficients.

5.2. Computational costs

Besides assessing the ability of both algorithms to track time-varying model coefficients, a simulation study is performed to compare the computational costs. The study estimates the time required by each agent and algorithm to calculate a new prediction after the central agent obtain a new data sample. To show the expected better scaling properties of the D-MIDAS, we estimated the computational time for an increasing learning network size of contracted agents. We again used simulated time series data that are generated with the previously introduced approach. However, instead of creating an AR(1)-, we used an AR(4)-process. In this study we performed online learning for 1 000 simulated time steps while recording the time it took to complete each operation. To achieve comparability between the Adaptive D-MIDAS and OADMM, the Adaptive D-MIDAS learned two models in parallel. For both algorithms, this resulted in an almost equal amount of data that was exchanged within the learning network. The simulation study was performed on a system with a i5-5200U CPU, 8 GB DDR3 RAM and a Windows 10 OS. Because both algorithms were used locally, we neglected the encryption and decryption steps of the Adaptive D-MIDAS. Hence, the observed performance gap in computational speed would decrease in case encryption was required to ensure data privacy.

Computational times are summarised in Figure 7. They were obtained by averaging the computational time for each and every one of the 1 000 time steps. The Adaptive D-MIDAS is faster than the OADMM overall. Furthermore, the algorithm shows a better scaling behaviour with respect to the learning network size. This is expected since, at each and every time t, the OADMM needs to solve a linear system of equations. Depending on the solving technique, complexity grows at least quadratically with the number of equations. The Adaptive D-MIDAS scales better because its updates are simple linear operations.

6. Case study

Our distributed and online learning algorithms were benchmarked on a real-world dataset of wind power generation for 311 sites. The dataset is a subset of the one used in Girard & Allard (2013). The temporal resolution is of 15 minutes and our subset covers 40 000 time steps, corresponding to 416 days. Figure 8 shows the location of the sites in Western Denmark. Many sites are located in close proximity to each other. This allows accounting for relevant spatial-temporal patterns when forecasting wind power generation for short lead times. To highlight the benefits of online learning, we benchmarked the forecasts from our

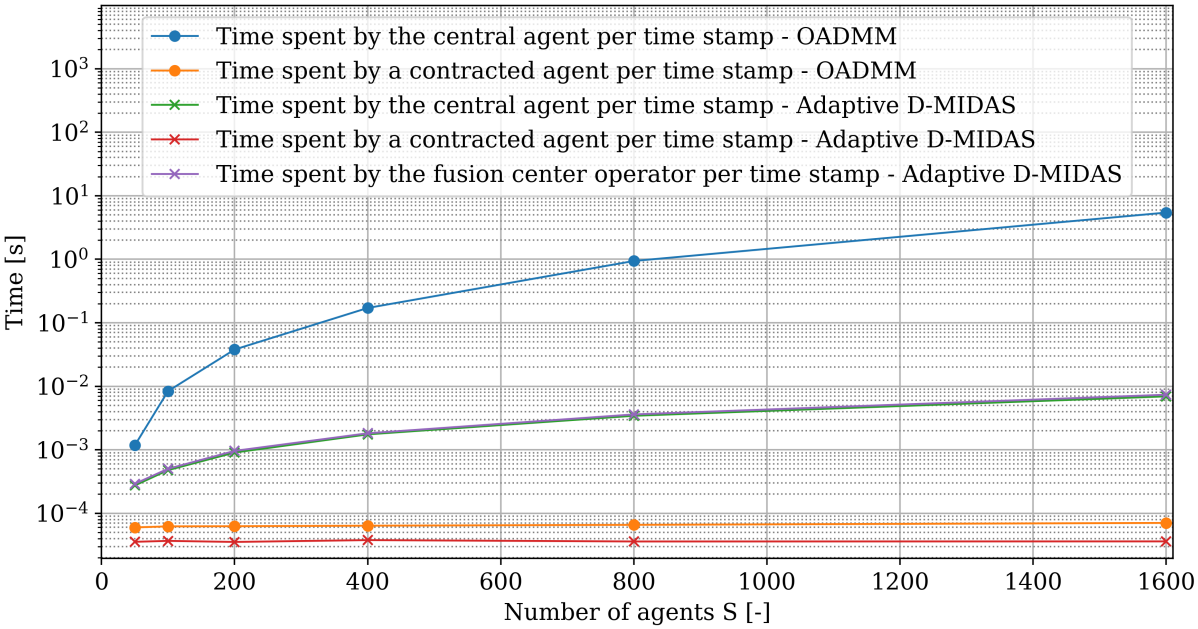

Figure 7: Average time (over 1 000 time steps) required by each agent to complete its tasks at a given time step, for both OADMM and Adaptive D-MIDAS approaches, as a function of total number of agents S.

online algorithms against those that would be otinaed from L_1-regularized AR-X models with time-invariant coefficients. The model coefficients were then estimated on the training part of the dataset only.

The benefits of exploring spatial-temporal patterns in wind power generation data have been shown for a different subset in Messner & Pinson (2019). The authors showed that high-dimensional regularised AR-X models outperform univariate AR models which only use on-site power measurements. All model coefficients were estimated in a time-varying fashion. Based on these results, we allowed ourselves to disregard univariate AR models with time-varying coefficients in our case study.

6.1. Data preprocessing

First, the raw data was normalised by dividing the time series of each site by the respective nominal capacity. Write $x_{s,t}$ the normalised wind power generation observed at time t and for site s. In addition, a logit-Normal transformation of the original time-series was considered, as proposed by Lau & McSharry (2010), i.e., at each and every time t and site s,

$$y_{s,t} = \ln\left(\frac{x_{s,t}}{1 - x_{s,t}}\right) , \quad \forall s, t \ . \tag{36}$$

To account for the bound effects, a coarsening approach was used (Pinson , 2012), for which values of 0 and 1 are set to 0.01 and 0.99, respectively.

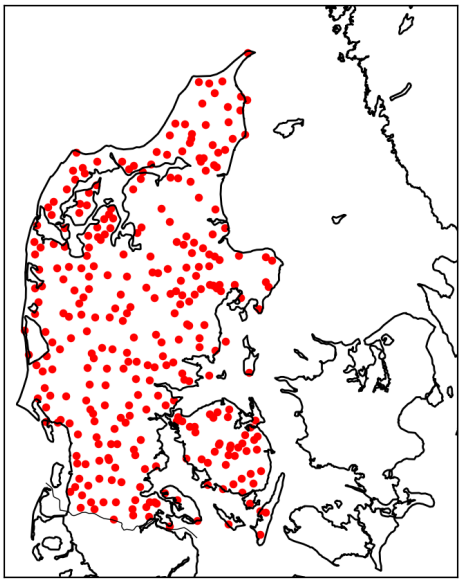

Figure 8: Location of sites in Western Denmark.

6.2. Case study setup

The data is split into two equal sub-periods of 20 000 time steps. The first part is used for training and hyperparameter optimisation, and the second for genuine out-of-sample forecast verification. Over the first period, the hyperparameters of all algorithms were optimized with a grid search scheme. After identifying suitable hyperparameters for the Adaptive D-MIDAS, the same hyperparameters were then applied to its communication-reduced version. The LASSO's L_1-regularisation parameter λ for the batch AR-X models was determined through 1-fold cross-validation. For both approaches, the forgetting factors are to be seen as variables that control how much of the past data is used for estimation. Hence, optimising these forgetting factors through cross-validation is to be seen as equivalent to determining an optimal training set size in the case of batch learning.

For a given site s, the Mean Absolute Error (MAE),

$$\text{MAE} = \frac{1}{T}\sum_{t=1}^{T}|y_{s,t} - \hat{y}_{s,t}| \tag{37}$$

and the Root Mean Squared Error (RMSE),

$$\text{RMSE} = \sqrt{\frac{1}{T}\sum_{t=1}^{T}(y_{s,t} - \hat{y}_{s,t})^2} \tag{38}$$

were used as performance metrics. To further quantify the performance of each model, the skill score I

$$I_S = 1 - \frac{S_{\text{Model}}}{S_{\text{Pers}}} \tag{39}$$

was used to assess the improvement over persistence forecasts (the latest observed power measurement is used as the next prediction), where S could be the metrics MAE or RMSE.

Owing to the large number of wind farms in the dataset, hyperparameter optimisation was performed for all wind farms at once, instead of for each site individually. A set of hyper-parameters was evaluated by considering the skill score distribution that contained the scores of all 311 sites. The median, the lower quartile and the inter-quartile range were used here as decision criteria. It was further decided to perform multi-step-ahead forecasting with up to 4 steps ahead. In general, different strategies exist for multi-step-ahead forecasting, where a good overview is presented in Ben Taieb *et al.* (2012). The most common approaches are either the iterative calculations of 1-step-ahead predictions or training separate models for each lead time. The iterative calculation of 1-step-ahead predictions results in the accumulation of forecast errors. Therefore, we used the direct approach and trained models for each lead time.

The hyperparameters of the Adaptive D-MIDAS and the batch AR-X model were optimized for each of the 4 lead times. Based on the significantly longer simulation times, the hyperparameters of the OADMM were optimized for 1-step-ahead predictions only. The selected hyperparameters were then applied for all other lead times. Due to the observed longer burn-in period of the Adaptive D-MIDAS, the performance metrics were calculated for both online algorithms only for the time steps between t =10 000 and t =20 000.

To obtain predictions for all sites of the dataset, each site took the role of the central agent once, while acting as a contracted agent in the other 310 simulations (i.e., for all other sites). Therefore, to obtain predictions for all sites and a single lead time, in total 311 AR-X models were estimated.

6.3. Results

Focusing first on hyperparameter optimisation, Figure 9 gives an example of the results obtained by optimizing the forgetting factor μ for the Adaptive D-MIDAS approach, when performing 1-step ahead forecasting. The boxplot shows the improvement over persistence forecasts for all 311 sites, as a function of the forgetting factor μ. Each box extends from the lower to the upper quartile (denoted Q_1 and Q_3, respectively), where the horizontal line indicates the median of the obtained RMSE skill score distributions. The maximum length of the whiskers is set to 1.5 times the interquartile range (Q_3-Q_1). The upper whisker then indicates the last sample which is found to be below or equal to the threshold of $Q_3+1.5(Q_3-Q_1)$. If a data point of the distribution is found outside this range, it is classified as an outlier and marked with a circle. The same concept applies to the lower whisker, which marks the first sample that is found to be within the range of $Q_1 - 1.5(Q_3 - Q_1)$.

A μ value of 0.95 performed slightly better than the remaining selected values when considering the aforementioned decision criteria. Therefore, this value was subsequently selected when performing online learning to estimate the performance on unseen data. The same approach was followed when tuning the other hyperparameters.

After finding suitable hyperparameters for both online algorithms, online learning was performed on the complete dataset. In contrast, the batch AR-X model coefficients were estimated over the first 20 000 time steps and then used to generate predictions over the

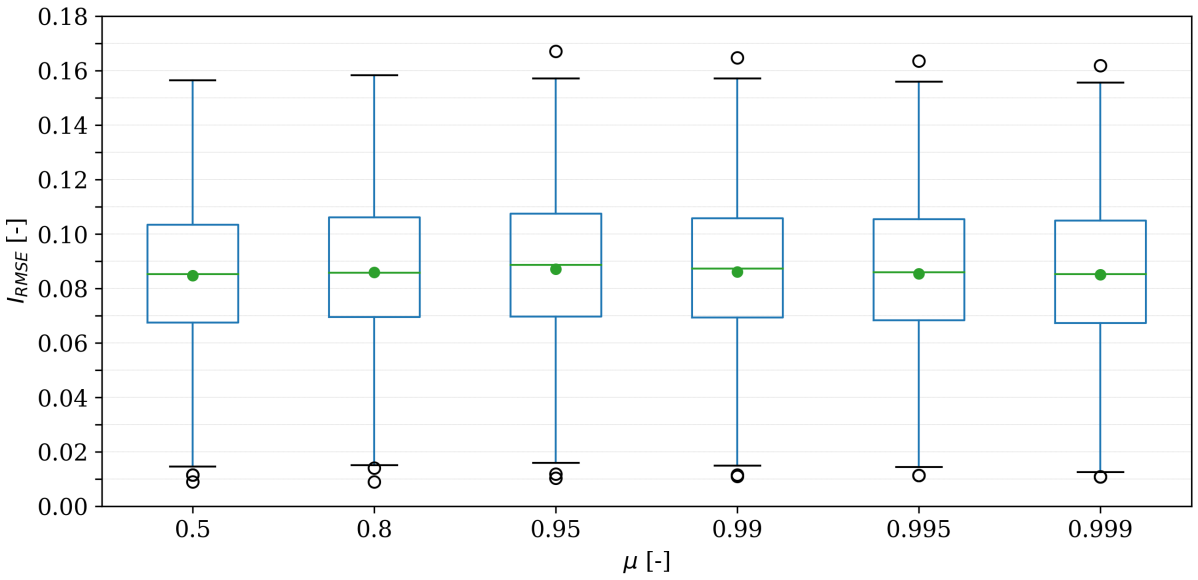

Figure 9: RMSE skill score of the Adaptive D-MIDAS with reference to the persistence forecast for 1-step ahead forecasts, as a function of the forgetting factor μ. The skill score values are computed for the time stamps $t = 10000$ to $t = 20000$.

remaining 20 000 time steps without re-estimating the model coefficients. Results are collated in Figure 10, for all approaches considered and for all sites, again with boxplots for skill score values (both in terms of RMSE and MAE).

Overall, all online distributed learning algorithms outperform the batch learning one (LASSO estimation in AR-X models), with the advantage that no data from contracted agents is actually shared with the central agents. A paired t-test supported the statistical significance by rejecting the null hypothesis of equal means at the 0.05 significance level. The number of outliers for the batch LASSO additionally emphasises the strength of online learning because the poor performance of batch estimation can be explained by the non-stationarity of the wind power generation time series. Hence, there are significant differences between the time-varying coefficients throughout the value period, and the coefficients estimated over and fixed at the end of the training period. Furthermore, when computing the bias it was observed that all forecasting models exhibit negligible bias values (not shown here).

The results further show that OADMM, despite being computationally more expensive, outperforms the Adaptive D-MIDAS for all lead times and skill scores. A paired t-test also supported the statistical significance of the results here. In addition, the performance gap increases for further lead times. This may be due to the structure and workings of both online algorithms. Indeed, the OADMM minimises the cumulative loss over all past observations where the covariance structures $\boldsymbol{H}_t$ and $\boldsymbol{p}_t$ carry the information of all previous samples. By varying the applied forgetting factor the number of past samples that are effectively used to update all algorithm parameters is controlled. As a result, even when

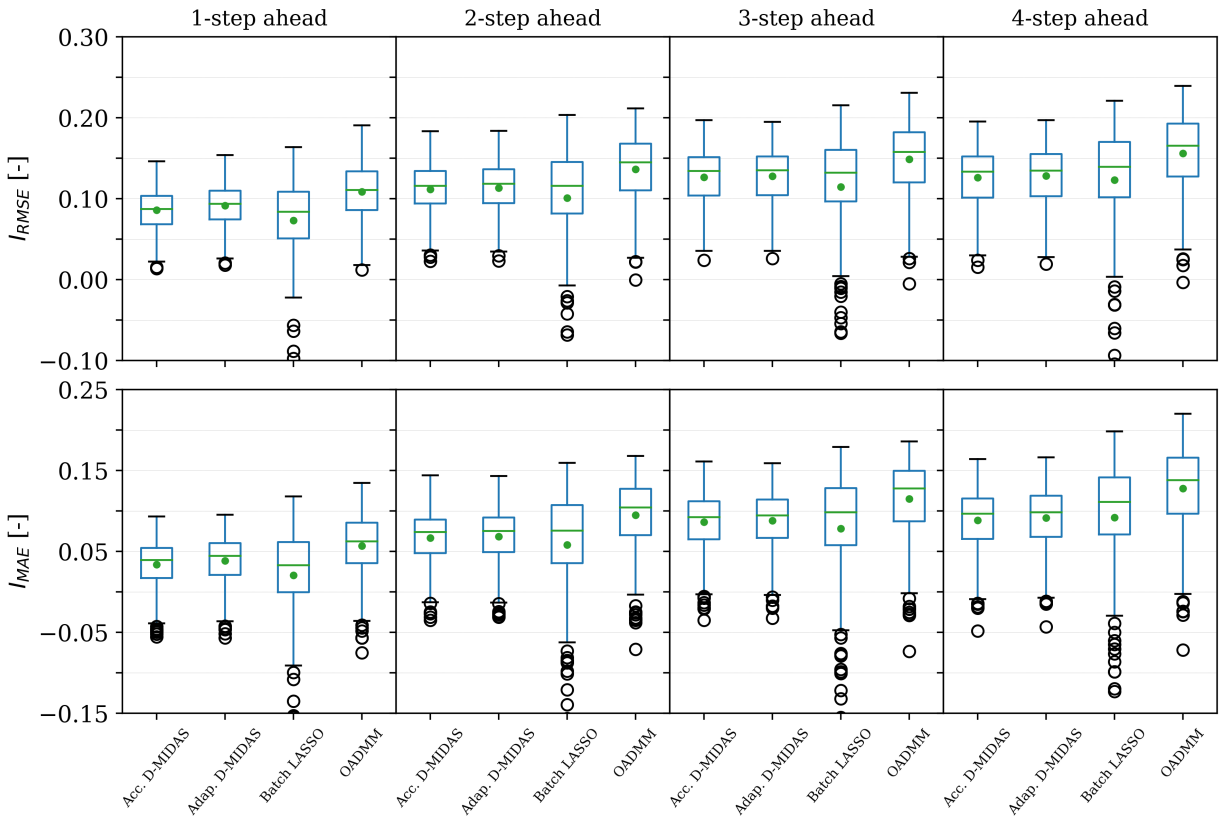

Figure 10: RMSE (top row) and MAE (bottom row) skill scores for the online distributed and batch learning approaches for different lead times. The skill score values are computed over the evaluation period, from $t = 20000$ to $t = 40000$. The dots indicate the mean of the skill score distributions.

a set of successive large forecast errors are observed, the estimated model coefficients are less subject to variations. The Adaptive D-MIDAS on the other hand does not utilize covariance structures to estimate model coefficients. Instead it uses the estimated gradient of the current squared loss between the observation and prediction to re-estimate the model coefficients. Therefore, large forecast errors directly translate to noticeable variations in the estimated model coefficients. A resulting shortcoming may be that the algorithm could be highly sensitive to outliers and structural breaks in the time series. While for 1-step-ahead predictions the model coefficient update is performed right after, i.e., naturally 1 time step after the prediction is made, for greater lead times there is a time lag because one must wait k steps to obtain the forecast error of a k-step-ahead forecast. This, paired with the sensitivity with respect to large forecast errors, may explain the lower forecast accuracy of the Adaptive D-MIDAS for further lead times. As mentioned earlier within the study on simulated data, the OADMM deals essentially better with this condition since the covariance structures carry an inertia whereby single or multiple large forecast errors do not affect the model coefficient estimates as much. Here it should be noted that this statement only holds for a sufficiently large forgetting factor.

Finally, one can verify that the communication-reduced Adaptive D-MIDAS version (Acc. D-MIDAS) does not perform significantly worse than the standard version. Thus, this version is an alternative in applications where re-estimating the model coefficients as quickly as possible has a high priority.

7. Conclusions

Two novel online distributed learning algorithms, the OADMM and Adaptive D-MIDAS, were proposed for high-dimensional AR-X model coefficient estimation to be used in wind power forecasting. The distributed component of both algorithms enables the estimation of AR-X models without the necessity of sharing sensitive data, such as power measurements, directly with other agents or entities. This enables competing wind farm operators to co-operate and collectively improve the forecasts for their sites. On the other hand, the online component allows the estimated model coefficients to follow the time-varying conditions of wind power generation time-series. Our main focus has been on distributed learning and forecasting for a class of linear models. Obviously then, the quality of the forecasts obtained is linked to the relevance of such linear models in practice. In view of the literature on short-term wind power forecasting, AR-X models are highly relevant for the lead times and forecasting setups considered in the paper. Some relevant generalisation could readily be considered e.g. to some types of regime-switching models (Self-Exciting Threshold Auto-Regressive – SETAR, and Smooth Transition Auto-Regressive – STAR). As long as the models involved are linear and separable, the methods discussed in the paper could be used in a similar manner. More broadly though, generalisation to nonlinear and more complex models may be more involved.

The OADMM relies on a LASSO-type objective function to estimate the coefficients of regularised AR-X models, in combination with an exponential forgetting factor to control the level of adaptivity. The algorithm minimises at any time t the cumulative loss over all observed samples (up to t), which requires the solving of a linear system of equations to update the algorithm parameters. Due to the non-negligible time for solving large equation systems, the Adaptive D-MIDAS is subsequently introduced. Owing to its design, all parameter updates are computationally cheaper to obtain. The algorithm is based on a mirror descent method where the gradient of the current squared forecast error is used to update dual variables. These are then mapped via a link function to the AR-X model coefficients. In addition, an accelerated version of the Adaptive D-MIDAS was proposed, i.e., a communication-reduced version. The algorithm achieves faster model coefficient re-estimates by using the dual variables from the previous time stamp. We verified that the impact on forecast accuracy is small.

A study on simulated data verified the ability of both algorithms to track time-varying model coefficients. However, the OADMM approach brings a better trade-off between adaptivity and limited variability of the estimated model coefficients, than the Adaptive D-MIDAS approach. Owing to its design, by minimising the cumulative loss over all past samples, large forecast errors do not directly cause large variations in the model coefficient estimates. The better controllability between adaptivity and the estimated model coeffi-

cient variance is the reason why the OADMM achieves a better forecast accuracy than the Adaptive D-MIDAS in the case study with a real-world dataset of 311 wind farms. The case study additionally confirmed that online learning is superior to offline learning, as already supported by previous work, although based on centralised learning algorithms.

Future works should address strategies to reduce the greater variability in the estimated model coefficients of the Adaptive D-MIDAS. Since we only considered deterministic forecasting models, future works should investigate extensions of the online distributed learning algorithms for the case of probabilistic forecasting. Then, besides other proposals for distributed online learning, and to relax the assumption such that agents are willing to collaborate, truthfully and rationally, it may be crucial to investigate federated learning and data markets. These new concepts may incentivise and support improvements in forecast quality when relevant data and features are distributed, both geographically and in terms of ownership.

Acknowledgements

Acknowledgements are due to Energinet.dk, the Transmission System Operator in Denmark, for the data used in this work. In addition, the authors are grateful to the editors and reviewers for their comments and suggestions which allowed improvement of the work presentation in that manuscript.

Appendix A. Algorithms

Algorithm 1 Online ADMM

Central agent decides on λ, ρ, ν and L. Initialize $\hat{\boldsymbol{\beta}}_{s,0}$, $\boldsymbol{z}_{s,0}$ and $\boldsymbol{u}_{s,0}$ for $s \in \Omega_s$, $\boldsymbol{H}_0$, $\boldsymbol{P}_0$ and t to be 0. To build $\boldsymbol{M}^\top \boldsymbol{M}$, contracted agents share $\boldsymbol{M}_s^\top \boldsymbol{M}_s$ with the central agent j.
while agents want to perform distributed online learning **do**
  $t := t + 1$
  $y_{s_j,t}$ is revealed to the central agent
  $\boldsymbol{H}_t := \nu \boldsymbol{H}_{t-1} + (\boldsymbol{a}_{t-1}\boldsymbol{M})^\top (\boldsymbol{a}_{t-1}\boldsymbol{M})$
  $\boldsymbol{p}_t := \nu \boldsymbol{p}_{t-1} + y_{s_j,t} (\boldsymbol{a}_{t-1}\boldsymbol{M})$
  Central agent updates $\boldsymbol{z}_{t-1}$ and distributes local values to contracted agents
  $\left(\boldsymbol{H}_t + \rho \boldsymbol{M}^T \boldsymbol{M}\right) \boldsymbol{z}_t = \boldsymbol{p}_t + \rho \boldsymbol{M}^\top (\hat{\boldsymbol{\beta}}_{t-1} + \boldsymbol{u}_{t-1})$
  $[\boldsymbol{z}_{s_1,t}, ..., \boldsymbol{z}_{s_S,t}] := \boldsymbol{z}_t$
  for $s \in \Omega_s$ **do**
    $\boldsymbol{u}_{s,t} := \boldsymbol{u}_{s,t-1} + \hat{\boldsymbol{\beta}}_{s,t-1} - \boldsymbol{M}_s \boldsymbol{z}_{s,t}$
    $\hat{\boldsymbol{\beta}}_{s,t} := \mathbb{S}_{\lambda/\rho} (\boldsymbol{M}_s \boldsymbol{z}_{s,t} - \boldsymbol{u}_{s,t})$
    Agent s uses latest observation $y_{s,t}$ to form $\boldsymbol{a}_{s,t}$
    $\widetilde{y}_{s,t+1|t} := \boldsymbol{a}_{s,t} \hat{\boldsymbol{\beta}}_{s,t}$
    share $\widetilde{y}_{s,t+1|t}$, $\boldsymbol{a}_{s,t}\boldsymbol{M}_s$ and $\boldsymbol{M}_s^\top \left(\hat{\boldsymbol{\beta}}_{s,t} + \boldsymbol{u}_{s,t}\right)$ with central agent
  end for
  $\hat{y}_{s_j,t+1|t} := \sum_{s \in \Omega_s} \widetilde{y}_{s,t+1|t}$
  Central agent j stacks local $\boldsymbol{a}_{s,t}\boldsymbol{M}_s$ and $\boldsymbol{M}_s^\top \left(\hat{\boldsymbol{\beta}}_{s,t} + \boldsymbol{u}_{s,t}\right)$
  $\boldsymbol{a}_t \boldsymbol{M} := [\boldsymbol{a}_{s_1,t}\boldsymbol{M}_{s_1}, ..., \boldsymbol{a}_{s_S,t}\boldsymbol{M}_{s_S}]$
  $\boldsymbol{M}^\top \left(\hat{\boldsymbol{\beta}}_t + \boldsymbol{u}_t\right) := \left[\boldsymbol{M}_{s_1}^\top \left(\hat{\boldsymbol{\beta}}_{s_1,t} + \boldsymbol{u}_{s_1,t}\right), ..., \boldsymbol{M}_{s_S}^\top \left(\hat{\boldsymbol{\beta}}_{s_S,t} + \boldsymbol{u}_{s_S,t}\right)\right]$
end while

Algorithm 2 Adaptive D-MIDAS

Central agent creates decryption key $\mathbb{K}^*$, selects a set of learning rates (collected in Ω_η) and shares both quantities with its contracted agents.
Initialize t and $\hat{\boldsymbol{\beta}}_{s,0}^{(\eta)}$, $\boldsymbol{\theta}_{s,0}^{(\eta)}$ for $s \in \Omega_s$ and $\eta \in \Omega_\eta$ to be 0. Additionally, initialize $CAE_{s_j}^{(\eta)}$ for $\eta \in \Omega_\eta$ to be 0. Central agent selects μ and p but only shares p with the fusion centre and contracted agents.
while agents want to perform distributed online learning **do**
    $t := t + 1$
    $y_{s_j,t}$ is revealed to the central agent
    for $\eta \in \Omega_\eta$ **do**
        $r_{t|t-1}^{(\eta)} := \hat{y}_{s_j,t|t-1}^{(\eta)} - y_{t,s_j}$
        $CAE_t^{(\eta)} = \mu CAE_{t-1}^{(\eta)} + |r_{t|t-1}^{(\eta)}|$
    end for
    Central agent encrypts forecast errors with $\mathbb{K}(\cdot)$ and shares them through the fusion centre with its contract agents
    for $s \in \Omega_s$ **do**
        Agent s decrypts forecast errors with $\mathbb{K}^*(\cdot)$
        for $\eta \in \Omega_\eta$ **do**
            $\boldsymbol{\theta}_{s,t}^{\eta} := \boldsymbol{\theta}_{s,t-1}^{(\eta)} - \eta \cdot \boldsymbol{a}_{s,t-1} r_{t|t-1}^{(\eta)}$
        end for
        Transmit list of dual vectors to fusion centre
    end for
    Fusion centre operator computes denominators of link function, $\gamma_t^{(\eta)}$
    for $\eta \in \Omega_\eta$ **do**
        $\boldsymbol{\theta}_t^{(\eta)} := \left[\boldsymbol{\theta}_{s_1,t}^{(\eta)}, ..., \boldsymbol{\theta}_{s_S,t}^{(\eta)}\right]$
        $\gamma_t^{(\eta)} := \|\boldsymbol{\theta}_t^{(\eta)}\|_p^{p-2}$
    end for
    Fusion centre operator shares $\gamma_t^{(\eta)}$ with all agents
    for $s \in \Omega_s$ **do**
        Agent s uses latest observation $y_{s,t}$ to form $\boldsymbol{a}_{s,t}$
        for $\eta \in \Omega_\eta$ **do**
            $\forall\ k,\ \hat{\beta}_{s,t,k}^{(\eta)} := \frac{\text{sign}\,(\theta_{s,t,k}^{(\eta)})|\theta_{s,t,k}^{(\eta)}|^{p-1}}{\gamma_t^{(\eta)}}$
            $\widetilde{y}_{s,t|t-1}^{(\eta)} := \boldsymbol{a}_{s,t} \hat{\boldsymbol{\beta}}_{s,t}^{(\eta)}$
            Each contracted agent shares partial predictions through fusion centre with central agent
        end for
    end for
    for $\eta \in \Omega_\eta$ **do**
        $\hat{y}_{s_j,t|t-1}^{(\eta)} := \sum_{s \in \Omega_s} \widetilde{y}_{s,t|t-1}^{(\eta)}$
    end for
    Central agent selects final prediction according to $\min_\eta MAE_{s_j}^{(\eta)}$
end while

References

Badi H. Baltagi, B. H., Fingleton, B. & Pirotte, A. (2014). Estimating and forecasting with a dynamic spatial panel data model. Oxford Bulletin of Economics and Statistics, 76, 112–138.

Beck, A. & Teboulle, M. (2003). Mirror descent and nonlinear projected subgradient methods for convex optimisation. Operations Research Letters, 31, 167–175.

Bekierman, J. & Manner, H. (2018). Forecasting realized variance measures using time-varying coefficient models. International Journal of Forecasting, 34, 276–287.

Ben Taieb, S., Bontempi, G., Atiya, A. & Sorjamaa, A. (2012). A review and comparison of strategies for multi-step ahead time series forecasting based on the NN5 forecasting competition. Expert Systems with Applications, 39, 7067–7083.

Bessa, R.J., Miranda, V., Botterud, A., Zhou, Z. & Wang, J. (2012). Time-adaptive quantile-copula for wind power probabilistic forecasting. Renewable Energy, 40, 29–39.

Boyd, S., Parikh, N., Chu, E., Peleato, B. & Eckstein, J. (2010). Distributed optimisation and statistical learning via the Alternating Direction Method of Multipliers. Foundations and Trends in Machine Learning, 3, 1–122.

Cavalcante, L., Bessa, R.J., Reis, M. & Browell, J. (2017). LASSO vector autoregression structures for very short-term wind power forecasting. Wind Energy, 20, 657–675.

Dowell, J. & Pinson, P. (2016). Very-short-term probabilistic wind power forecasts by sparse vector autoregression. IEEE Transactions on Smart Grid, 7, 763–770.

Duchi, J. & Shalev-Shwartz, S. & Singer, Y. & Chandra, T. (2008). Efficient projections onto the l_1-ball for learning in high dimensions. International Coference on Machine Learning, 272–279.

Giebel, G. & Kariniotakis, G. (2017). Wind power forecasting - a review of state of the art. In: Renewable Energy Forecasting – From Models to Applications (Ed. Kariniotakis, G.), 59–96.

Girard, R. & Allard, D. (2013). Spatio-temporal propagation of wind power prediction errors. Wind Energy 16, 7, 999–1012.

He, M., Yang, L., Zhang, J. & Vittal, V. (2014). A spatio-temporal analysis approach for short-term forecast of wind farm generation. IEEE Transactions on Power Systems, 29, 1611–1622.

Kou, P., Gao, F. & Guan, X. (2013). Sparse online warped Gaussian process for wind power probabilistic forecasting. Applied Energy, 108, 410–428.

Lau, A. & McSharry, P. (2010). Approaches for multi-step density forecasts with application to aggregated wind power. Annals of Applied Statistics, 4, 3, 1311–1341.

Li, X., Chen, J., Liu, W., Wan, W. (2009). An improved AES encryption algorithm. IET International Communication Conference on Wireless Mobile and Computing (CCWMC 2009), 694–698.

Matamoros, J. (2017). Asynchronous online ADMM for consensus problems. Proc. of the 2017 IEEE International Conference on Acoustics, Speech and Signal Processing (ICASSP 2017), 5875–5879.

Matos, M., Bessa, R., Botterud, A. & Zhou, Z. (2017). Forecasting and setting power system operating reserves. In: Renewable Energy Forecasting – From Models to Applications (Ed. Kariniotakis, G.), 279–305.

Mazzi, N. & Pinson, P. (2017). Wind power in electricity markets and the value of forecasting. In: Renewable Energy Forecasting – From Models to Applications (Ed. Kariniotakis, G.), 259–278.

Messner, J.W. & Pinson, P. (2019). Online adaptive lasso estimation in vector autoregressive models for high-dimensional wind power forecasting. International Journal of Forecasting, 35, 1485–1498.

Min, W. & Wynter, L. (2011). Real-time road traffic prediction with spatio-temporal correlations. Transportation Research C, 19, 606–616.

Møller, J. K., Nielsen, H. A. & Madsen, H. (2008). Time-adaptive quantile regression. Computational Statistics & Data Analysis, 52, 1292–1303.

Nemirovski, A. S. & Yudin, D. B. (1983). Problem complexity and method efficiency in optimisation. Wiley.

Langford, J. & Lihong, L. & Zhang, T. (2009). Sparse online learning via truncated gradient. Journal of Machine Learning Research,10, 777-801.

Paci, L., Gelfand, A. E. & Holland, D. M. (2013). Spatio-temporal modelling for real-time ozone forecasting. Spatial Statistics, 4, 79–93.

Pinson, P. (2012). Very short-term probabilistic forecasting of wind power with generalized logit-Normal distributions. Journal of the Royal Statistical Society C, 61, 555–576.

Pinson, P. (2016). Introducing distributed learning approaches in wind power forecasting. Proc. of the 2016 International Conference on Probabilistic Methods Applied to Power Systems (PMAPS 2016).

Pinson, P. & Madsen, H. (2012). Adaptive modelling and forecasting of wind power fluctuations with Markov-switching autoregressive models. Journal of Forecasting, 31, 281–313.

Shalev-Shwartz, S. & Tewari, A. (2011). Stochastic methods for L1-regularized loss minimisation. Journal of Machine Learning Research, 12, 1865–1892

Sigrist, F, Künsh, H. R. & Stahel W. A. (2012). A dynamic nonstationary spatio-temporal model for short term prediction of precipitation. Annals of Applied Statistics, 6, 1452–1477.

Suzuki, T. (2013). Dual averaging and proximal gradient descent for online Alternating Direction Multiplier Method. Proc. of the 30th International Conference on Machine Learning (ICML), 28, 392–400.

Tastu, J., Pinson, P., Kotwa, E., Madsen, H. & Nielsen, H. A. (2011). Spatio-temporal analysis and modelling of short-term wind power forecast errors. Wind Energy, 14, 43–60.

Tastu, J., Pinson, P., Trombe, P.J. & Madsen, H. (2014). Probabilistic forecasts of wind power generation accounting for geographically dispersed information. IEEE Transaction on Smart Grid, 5, 480–489.

Wang, H. & Banerjee, A. (2012). Online alternating direction method. Proc. of the 29th International Conference on Machine Learning (ICML).

Zhang, Y. & Wang, J. (2018). A distributed approach for wind power probabilistic forecasting considering spatio-temporal correlation without direct access to off-site information. IEEE Transactions on Power Systems 33, 5, 5714–5726.